Journal of Atmospheric and Ocean Science
Vol. 10, No. 2, June 2005, 123–143

Taylor & Francis
Taylor & Francis Group

Interannual variability in the 1990s in the northern Atlantic and Nordic Seas

G. R. BIGG*†, S. R. DYE‡ and M. R. WADLEY§

†Department of Geography, University of Sheffield, UK
‡Centre for Environment, Fisheries and Aquaculture Science, Lowestoft, UK
§School of Mathematics, University of East Anglia, UK

(*Received 21 February 2005; in final form 13 July 2005*)

A global fine resolution curvilinear ocean model, forced by NCEP Re-Analysis fluxes, is used to study changes in the circulation of the Nordic Seas and surrounding ocean basins during 1994–2001. The model fields exhibit regionally distinct temporal variability, mostly determined by atmospheric forcing but in regions of significant sea-ice longer timescale variability is found. Some abrupt circulation changes accompany the relaxation of the westerlies following the peak North Atlantic Oscillation Index phase of the mid 1990s. The Greenland gyre spins up over the following years, with the increased circulation partially exiting through the Denmark Strait into the northern Atlantic as well as re-circulating within the Nordic Seas. This resulted in a distinct freshening around northern Iceland and an increase in the East Icelandic Current. However, these latter increases steadied after 1998, as the increased Greenland Sea gyre circulation led to a greater proportion of water leaving through the Denmark Strait, rather than re-circulating. The model Denmark Strait Outflow therefore doubles during the latter half of the 1990s. Increased convection in the Icelandic Sea in the model in 1998–2001 acted to obliterate the anomalies that would otherwise have fed into the East Icelandic Current. A fresh, cold anomaly from the Arctic during 1998/1999 is shown to propagate through the system. Model and observations show good agreement generally, but diverge at depth more in the last few years of the simulation. The model shows that density anomalies within the East Greenland Current do not exclusively derive from the Arctic but may also arise from air–sea interaction within the Greenland Sea. Convection is a major means of limiting anomaly propagation within the model. The contrast of climatological with daily forcing shows the inherent strength of the variability in the ocean circulation on sub-decadal timescales.

Keywords: Ocean modelling; Air–sea interaction; Ocean convection; Norwegian-Greenland Sea; East Icelandic Current

1. Introduction

Recent decades have seen significant variability in the properties and circulation of the northern Atlantic Ocean. In tune with the decadal-scale variability of the

*Corresponding author. Email: grant.bigg@sheffield.ac.uk

Journal of Atmospheric and Ocean Science
ISSN 1741–7538 print/ISSN 1741–7546 online © 2005 Taylor & Francis
http://www.tandf.co.uk/journals
DOI: 10.1080/17417530500282873

atmosphere's North Atlantic Oscillation (NAO) there has been a major movement in the location and strength of the deepest ocean convection in the northern Atlantic. During the 1960s and early 1970s winter-time convection reached the bottom of the Greenland Sea (Malmberg and Jonsson 1997) while in the Labrador Sea it was restricted to the upper 1000 m (Dickson *et al.* 2002). Following 1972, ocean convection in the Labrador Sea reached 1600 m and deepened gradually, but not monotonically, until the extreme winters of 1993 and 1994, when convection reached 2300 m (Lazier *et al.* 2002). In contrast, Greenland Sea convection was much reduced, reaching only the shallow depth of 800 m in 1994 (Lherminier *et al.* 1999). Following the abrupt reversal of the NAO in the winter of 1995–1996 there is evidence that the convection cells have switched back to their earlier mode. Labrador Sea convection has shallowed to order 1000 m (LabSea Group 1998, Lazier *et al.* 2002), and decreased in strength from about 9 Sv prior to 1995 to 2 Sv in the later 1990s (Rhein *et al.* 2002), while at least some localised convection within small-scale eddy features has occurred in recent years in more than one location in the Greenland Sea, to 2200 m in one location (Gascard *et al.* 2002) and in excess of 2400 m in another (Wadhams *et al.* 2002).

Nevertheless, the ocean's behaviour has not been purely determined by the atmosphere as significant changes in hydrographic and sea-ice regimes have also occurred during this time. Within the deeper regions of the Labrador Sea, beneath even the convection of the early 1990s, the water derived from Denmark Strait Overflow Water (DSOW) has tended to cool and freshen since the early 1970s (Lazier *et al.* 2002), although with some temporary reversals in both trends in the 1990s (e.g. Dickson *et al.* 2002). Within the Labrador Sea Water (LSW), over 1–2000 m, a cooling and freshening caused by mixing of the surface and existing LSW properties ceased in the mid-1990s as this layer became disconnected from the surface. Indeed, both the salinity and temperature increased during the late 1990s, due to mixing from the boundaries of the Labrador Sea into the central waters (Lazier *et al.* 2002) rather than from *in situ* convection. The near-surface Labrador Sea exhibited this warming but little change in salinity (Lazier *et al.* 2002).

The deeper Atlantic south of the Greenland–Iceland–Scotland (GIS) Ridge has tended to freshen over recent decades (Dickson *et al.* 2002), although the 1990s saw less regular behaviour. Indeed the salinity of the deeper waters of the Icelandic Basin actually rose during this time. The deep waters issuing from the Denmark Strait also showed a temporary salinification and warming around 1997–1998, and again in 2001. Near the surface, the Irminger Sea has warmed and salinified during the latter half of the 1990s (Reverdin *et al.* 1999), possibly in response to the less cyclonic behaviour of the atmosphere.

The deeper anomalies in the northern Atlantic have their origin in the upstream basins of the Nordic and Arctic seas. The water properties of these basins, in turn, are determined by the local air–sea fluxes but also from the interplay of the upper ocean Atlantic Water (AW) flowing into and through the Norwegian Sea, the exchange through the Fram Strait and the deep exchange between the Greenland and Norwegian Sea basins. The influx of AW through the Faroe-Shetland Channel is largely linked to the decadal-scale variation of the NAO (Dye 1999) and so was at a maximum during the late 1980s to early 1990s (Furevik 2001), decreasing during the late 1990s (Orvik *et al.* 2001, Karcher *et al.* 2003). There is some evidence for an increase in inflow again from 2000 (Karcher *et al.* 2003). These anomalies can be traced at reduced amplitude into the Arctic, through the outflow regions of the Barents Sea and Fram Strait (Furevik 2001).

The Fram Strait is the major export route for sea-ice from the Arctic. This shows significant decadal-scale variability (Schmith and Hansen 2003) but no long-term trend. In recent decades the 1950s and 1990s showed maximum efflux of ice, and hence freshwater (Vinje 2001), but interannual variability is large (Arfeuille *et al.* 2000, Dickson *et al.* 2002). Within the Greenland Sea, reduced Fram Strait ice flux is reflected in reduced sea-ice extents. Thus, during 1994 and 1995 there was much reduced sea-ice in the Greenland Sea (Toudal 1999) and the Odden Tongue off eastern Greenland did not form, but in 1997 the latter was at its most extensive and persistent (Comiso *et al.* 2001). Later years have seen this increase in Greenland Sea sea-ice persist, with the ice tending to thicken (http://polar.wwb.noaa.gov/seaice/Historical.html).

Within the deep waters of the Nordic Seas there has been a warming trend since the early 1980s following the shut down of convection 10 years earlier. This has been caused by increased horizontal exchange with the relatively warm Atlantic layer of the Arctic (Østerhus and Gammelsrød 1999). The Greenland Sea interior warmed first, followed by the Norwegian Sea at 2000 m from 1987, and shallower depths a few years later. This warming halted during 1993–1995 in the Norwegian Sea. Subsequently, by 1997, it increased in temperature by a further 0.02°C below 2000 m (Østerhus and Gammelsrød 1999). This interruption in Norwegian Sea warming was ascribed to a reversal in the flow in the Jan Mayen Channel as convection in the Greenland Sea reached its minimum. The decrease in transport of convected water from the Greenland Sea into the Norwegian Sea has seen the Norwegian Sea Deep Water (NSDW) thickness decreasing, so that the water outflowing through the FSC is no longer directly connected to the NSDW. This has resulted in a gradual freshening of this outflow, reflected in downstream conditions (Turrell *et al.* 1999).

As we have seen, the evolution of oceanic properties in the Nordic Seas and northern Atlantic is complicated by many factors. Particularly in the last decade there have been significant anomalies propagating through the system, but also large interannual variations. The atmosphere has experienced some of the most extreme opposite states of the NAO during this time, and remains in an unusual state, as shown by the many recent major flood events and droughts in western Europe. In this article we explore some of the links between the atmospheric forcing and the oceanic response, both short and intermediate term, through studying the results of a global ocean model, with enhanced North Atlantic and Arctic resolution, forced by daily atmospheric forcing from the NCEP re-analysis project during 1994–2001, and comparisons with observations in the vicinity of the Nordic Sea, where the model has its finest resolution. In the next section we describe the model and forcing data used. This is followed by an analysis of the model results and comparisons with observational data. Finally we address the causes of the model's successes and failures in the Nordic Sea area, closing with some comments on the role of the Denmark Strait in anomaly propagation within the East Greenland Current.

2. Model details

The global ocean general circulation model (OGCM) is a finer resolution version of the global curvilinear coordinate system model, developed by

Wadley and Bigg (2000), whose North Pole location is in Greenland. It is based on the Bryan–Semtner–Cox model; the base model equations are given in Beare (1998). The model has a free surface formulation for the barotropic mode (Webb 1996) and 19 levels in the vertical, varying in thickness from 30 m at the surface to 500 m at depth. Tracer (salinity and temperature) mixing has components in the horizontal, vertical and along isoneutral surfaces (Griffies *et al.* 1998). The values of the mixing coefficients are taken from England (1993), with the exception of the horizontal mixing coefficient, which was decreased to $1 \times 10^8\,m^2\,s^{-1}$. Note that the horizontal momentum diffusivity varies with grid resolution (Wadley and Bigg 2002). The near-surface vertical mixing uses the scheme of Philander and Pacanowski (1986). The topography is constructed from the ETOPO (1986) dataset, with the sill depths taken from Thompson (1995). A one-layer thermodynamic sea-ice model, based on Parkinson and Washington (1979), is coupled to the OGCM, with advection of sea-ice being driven by the surface ocean current, in a similar manner to the sea-ice within the Meterological Office's HadCM3 coupled model. Our model has been run at coarser resolution for several thousand model years and produces realistic sea-ice fields (Wadley and Bigg 2002). The model was also run at high resolution without sea-ice dynamics. There was only difference in the detail between the thermodynamic-only and thermodynamic + dynamics runs. Most of the model results in the main focus area of this study, in the Nordic Seas, are therefore not strongly controlled by sea-ice advection from the Arctic, as we see later.

Placing the model's North Pole in Greenland enhances the model resolution in the North Atlantic and Arctic considerably. Thus, in the far field the model horizontal resolution is $2^\circ \times 1.5^\circ$ while in the Nordic Seas and Arctic the resolution is 0.5° or less (figure 1). Time-step length is a function of grid spacing, to allow efficient integration of the variable resolution grid (Wadley and Bigg 2000), with the coarsest time-step being 2700 s and the shortest, along the Greenland coast, being an eighth of this.

The OGCM was spun-up prior to the 1994–2001 NCEP-re-analysis forcing being applied. For the first year the model was globally relaxed at all depths, with a 30 day timescale, to the climatological temperature (Levitus *et al.* 1994) and salinity (Levitus and Boyer 1994). The surface wind stress applied was taken from the climatology of Hellerman and Rosenstein (1983). Robust relaxation continued for another 2 years, with relaxation below 1000 m lessened to a timescale of 360 days. A further 3 years of purely surface relaxation followed. By this stage the model had reached near surface equilibrium, although the sea-ice model had not yet been added. The model was then run until the end of year 21 using monthly mean freshwater fluxes from the climatology of Oberhuber (1988). No runoff was included. The heat flux used in this period of the spin-up was derived from restoring to an apparent atmospheric temperature, T^*, with a thermal coupling strength of $15\,Wm^{-2}\,K^{-1}$ using the heat flux climatology of Oberhuber (1988) as a starting point (see Wadley and Bigg (2002) for more details).

A control run was continued for another 9 years using this climatological forcing (henceforth called CONTROL). In addition, daily average NCEP re-analysis (Kalnay *et al.* 1996) wind stress, freshwater flux and heat flux data were used to simulate the years 1994–2001 (this run will be called DAILY). For post-March 1997 values the revised data provided on the NCEP web-site in 2002 were used. The heat flux for the model was derived from the sum of the surface solar, latent heat, long-wave and sensible heat fluxes. The latent heat flux was combined with

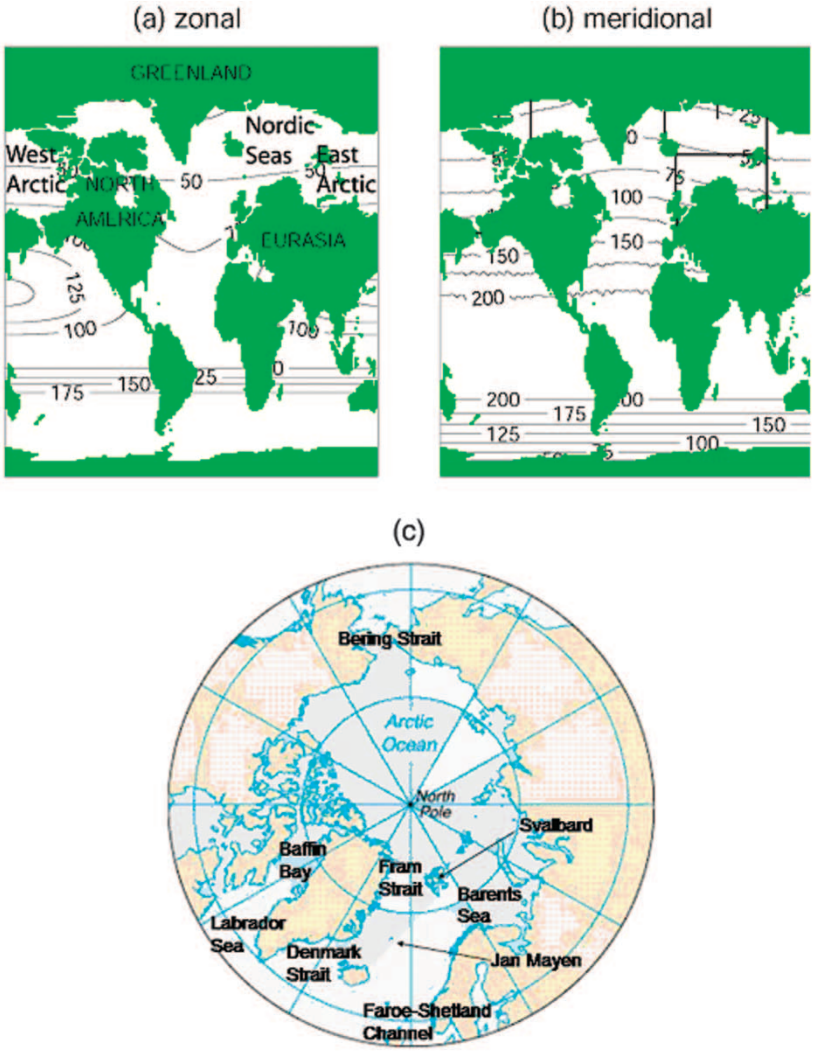

Figure 1. (a) Zonal and (b) meridional grid spacing in the projection. Note the resolution improves markedly as the grid enters the northern Atlantic, Arctic and Nordic Seas. The contour interval is 25 km. The thick solid lines in (b) show the sections used to calculate the various volume transports. In (c) the main straits and regions of interest in the article are shown.

the precipitation rate field to produce a net freshwater balance for the ocean surface. To allow for a transition from monthly to daily timescales in forcing, the year 1994 was run twice, with a ramping in of the forcing magnitude during the first realisation. The response of the Southern Hemisphere in the OGCM to the daily heat and freshwater flux forcing was not robust, with significant anomalies developing in the eastern Pacific, eastern Indian Ocean and tropical Atlantic. However, in the Northern Hemisphere such anomalies did not occur. As the regions affected were sufficiently far from the area of interest in the Northern Atlantic the freshwater and heat fluxes, but not the wind stress, south of 20°N were zonally averaged, with a 10° transition band between zonally averaged and full fluxes. A reasonable seasonal cycle then existed in the "daily" forcing years around the globe. It could be argued that the NCEP mean fields should have been used to spin-up the model, rather than earlier climatology. However, such an experiment was carried out and the representation of the global ocean at the end of the same 21 year spin-up was very poor (for example many ocean currents, and the Atlantic overturning, were only about half the strength suggested by observations; temperature and salinity fields were also poorly reproduced). It was therefore decided to use the older climatological forcing for the spin-up and accept the delay in deep water flows reflecting the effects of the switch to 1990s surface forcing.

3. Model results

3.1. *Basin-scale model variability*

Almost all variables examined in CONTROL, forced by the monthly varying climatological fields, had regular annual cycles without significant drift during the years corresponding to the DAILY run. In the latter, variables examined in the Southern Hemisphere showed some minor drift remaining even after the imposition of zonally averaged daily forcing. However, the predominant signal in the northern Atlantic and Arctic is a response to interannual variability. In only a few variables is drift observed and as we will see the most likely reason for this is related to abrupt change during the mid 1990s in the NCEP forcing. There are distinct differences in the frequency response of DAILY compared to CONTROL. The base seasonal variation is similar but the amplitude variation in DAILY can be much greater, as the latter captures daily variance and so the seasonal extremes (Killworth 1995). Figure 2(a) shows the Atlantic Overturning streamfunction for DAILY. The amplitude of the seasonal cycle is only about 1 Sv, very similar to that in CONTROL, but the variance is large with instantaneous values ranging 15–60 Sv. This large range is unimportant for the longer term, as it occurs because of the high frequency variability of the winds, and so the upper ocean currents, on this daily timescale. A better idea of variability is given in figure 2(b), where the monthly mean timeseries is given (thin line). Over our eight years the range is 21–37 Sv, with intermonthly variation typically only 2–4 Sv. For comparison, recent measurements of northward flow through the Faroe-Shetland Channel, a major component of the overturning circulation, shows monthly variation of up to 50% of the mean (Østerhus *et al.* 2005).

The variability, on atmospheric synoptic system timescales, is common to most variables, as is the tendency for the extremes to occur during the winter. Figure 2(a) also shows behaviour exhibited by some other, but not all, North Atlantic flow variables, in that a trend becomes evident from 1997 onwards. This post-1997 trend is more apparent in northern regions and is absent from the sub-tropical gyre for instance. Reasons for this trend will be explored later. The impact of the imposition of daily forcing is seen in figure 2(b), where the Atlantic overturning streamfunction in the CONTROL experiment is shown. It is seen that the decadal-scale change in figure 2(a) is not part of any CONTROL drift.

As well as expected differences in the frequency of variability there are also differences in the mean strength of basin-scale flow properties. The maximum

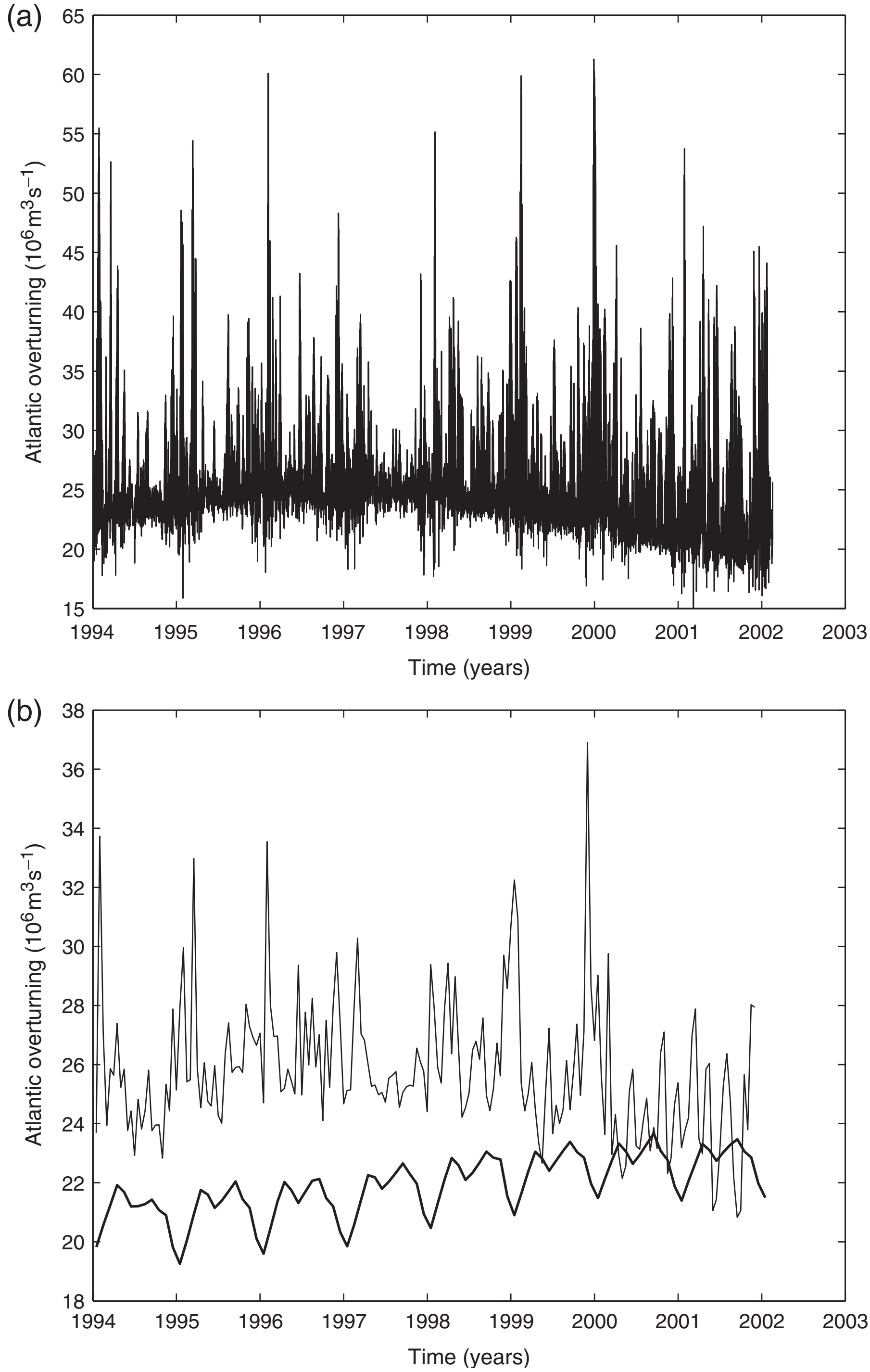

Figure 2. The Atlantic overturning streamfunction, in Sv or $10^6\,m^3\,s^{-1}$. (a) DAILY, shown at daily frequency; (b) CONTROL, shown at monthly frequency; the monthly mean DAILY timeseries is shown (thin line) for comparison.

Atlantic Overturning streamfunction varies between 19 and 21 Sv in CONTROL through the year; in DAILY the mean increases from roughly 24 to 26 Sv during the mid 1990s but then declines to around 22–23 Sv by 2001. Thus, through most of the period of interest it is 10–20% stronger than climatology would suggest, although reaching CONTROL levels by 2001. In contrast, the horizontal circulation of the North Atlantic sub-polar and sub-tropical gyres is generally weaker in DAILY. The climatological North Atlantic sub-tropical gyre of CONTROL has a mean of ~32 Sv, while in DAILY the interannual amplitude changes in the range 20–28 Sv, being lowest in 1995 and 2001. The North Atlantic sub-polar gyre CONTROL mean is ~22 Sv, similar to that in DAILY during 1994–1995, but the latter drops to ~16 Sv by 1999. This mean then persists until the end of the integration. The balance between horizontal and vertical motion in the North Atlantic is therefore different between the two runs. Vertical motion is of greater importance relative to horizontal advection for 1990s daily timescale forcing compared to climatological forcing. Of course, the latter is more representative of earlier decades and so we may be seeing a real inter-decadal change in model circulation rather than behaviour purely dependent on the switch to higher frequency variability in the forcing.

3.2. *The modelled Nordic Seas and environs*

The mean DAILY velocity fields at approximately 50 m (level 2) and 800 m (level 9) are shown in figure 3 north of about 20°N. Figure 1(b) shows the locations of a number of model sections that were used to monitor change in the Nordic Seas and environs during the 1990s. This may be related to the real map of the Arctic area shown in figure 1(c). These fluxes show a variety of behaviours.

The fluxes of the waters entering the system (that is, the Bering Strait and the Atlantic Water entering the Nordic Sea between Iceland and Scotland, figure 4) exhibit interannual variability but no trend. However, many flux sections within the Arctic and Nordic Seas, including those monitoring water leaving the system, do show a distinct trend, initiated after a period of stability during 1994–1995 (figure 5). The trend is for more water to leave the Arctic system through the Denmark Strait (about 2 Sv in total, or a doubling of the 1994–1995 total volume flux), balanced by a small decline in the deep outflow through the Faroe-Shetland Channel (~0.5 Sv) and a larger decline in the flux southward through the Labrador Sea and Baffin Bay. These trends continue throughout the remainder of the model simulation. In the Greenland Sea an additional interannual timescale is seen. The tendency for an increasing upper ocean flux out of the Arctic through Fram Strait, analogous to the trend above, halts in late 1997, with this flux stabilising (figure 5). The change in behaviour occurs later further downstream in the East Greenland Current and East Icelandic Current (into 1999, figure 6), but does not enter the Denmark Strait, where the flow continues to strengthen (figure 5). The post 1998 variability is also different downstream. The East Greenland Current shows a steep decline in flux, accentuated with depth; the East Icelandic flux shows only a cessation of the pre-1998 trend, but just at depth. Complicating the pattern in the Greenland Sea is a pre-1998 increase in the West Spitzbergen Current, directly reflected in more warm, Atlantic Water entering the Arctic through Fram Strait at depth. This trend ceases around 1998, but with a greater proportion of the increased West Spitzbergen flux entering the Greenland Sea gyre

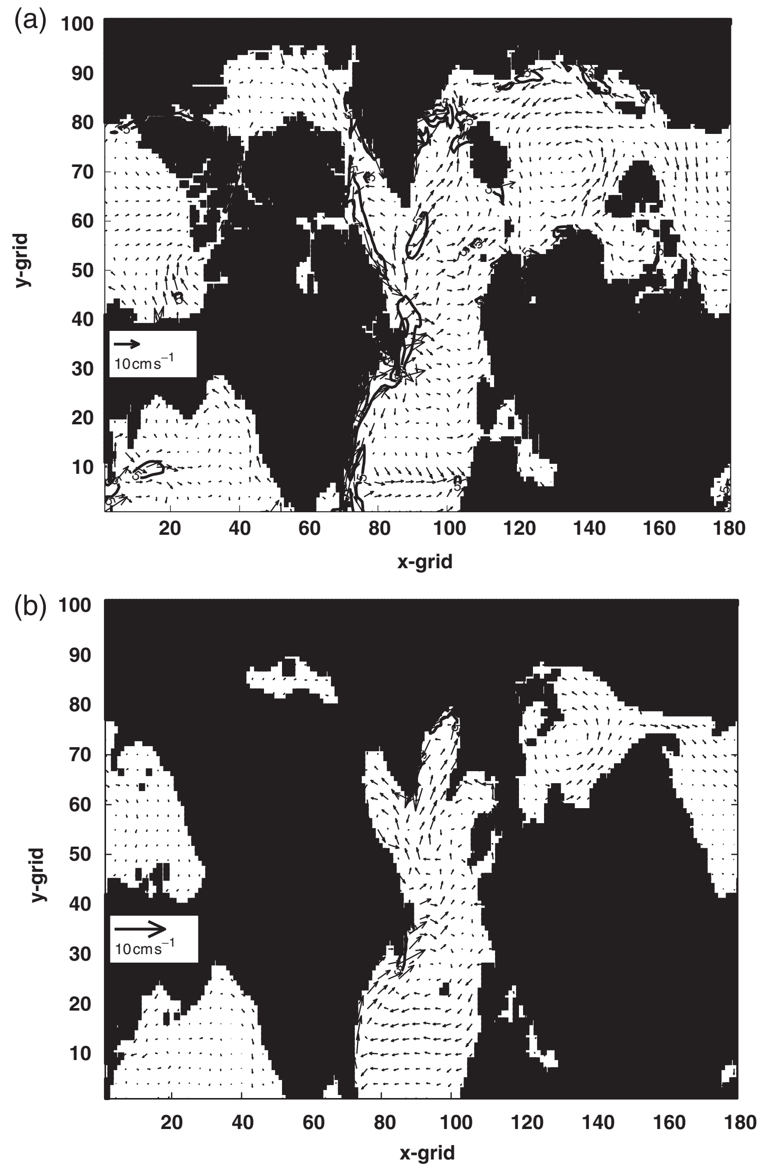

Figure 3. Mean horizontal velocity, averaged from seasonal snapshots, north of ~20°N at (a) 50 m (level 2), and (b) 800 m (level 9). In both, only every third gridpoint is shown.

than exited into the Arctic pre-1998. The overall impression is of the Greenland Sea Gyre spinning up during the mid 1990s and then moving to a new circulatory mode with water moving south tending to sink through its passage around the Gyre, largely through increased convection in the Icelandic Sea, but a greater proportion exiting the Greenland Sea through the Denmark Strait. Figure 7 shows a schematic of this series of changes.

In the other basins adjacent to the North Atlantic, the Norwegian gyre changes relatively little over 1994–2001, with a small decline in deep outflow through the

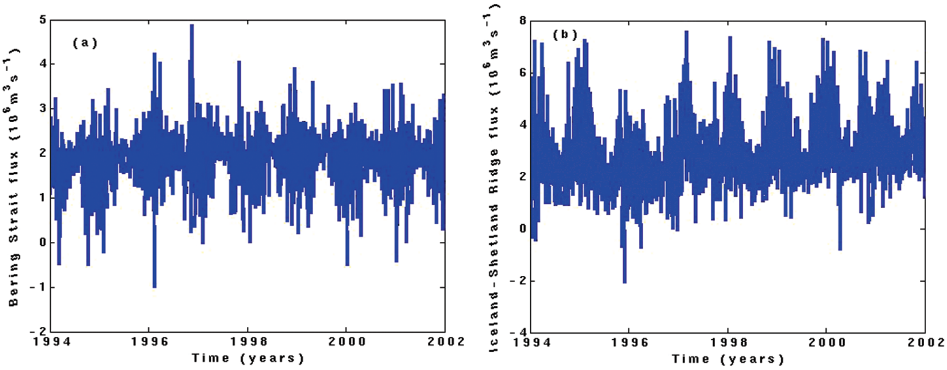

Figure 4. Timeseries plots of the total volume flux (Sv) entering the Arctic/Nordic Seas through (a) the Bering Strait and (b) across the Iceland–Shetland Ridge. Most of the flow in (b) is through the Faroe-Shetland Channel. Data is shown at daily frequency.

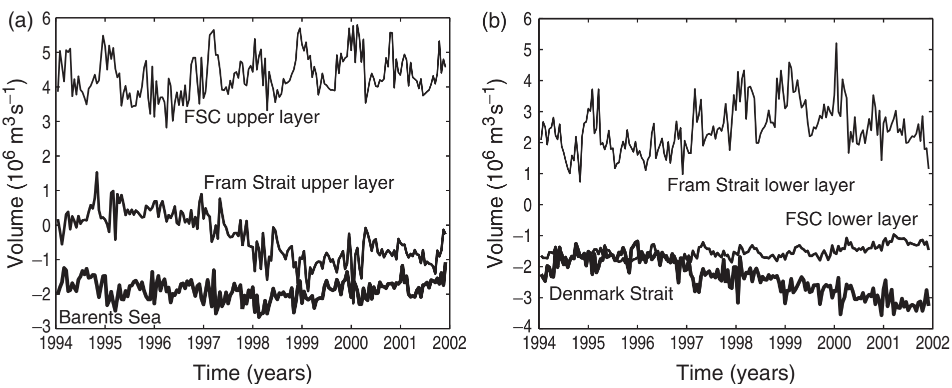

Figure 5. Timeseries plots of the (a) inflow into, and (b) outflow from, the Nordic Seas (Sv). Data is shown with a 1 month running mean. In (a) the negative Barents Sea value denotes outflow from the Arctic, just as the positive deep Fram Strait value in (b) denotes flow into the Arctic. See figure 1(b) for the orientation of the sections. Note that the depth separating upper from deep layers in Fram Strait is ~150 m, while in the Faroe-Shetland Channel (FSC) it is ~500 m.

Faroe-Shetland Channel. This is possibly traceable to a reversal of the deep water outflow through the Jan Mayen Channel from the deep Greenland gyre, which began in the middle of 1996 (figure 8). Note that the flow through the Jan Mayen Channel in the first three years of the simulation is only intermittent, as suggested by Bourke *et al.* (1993) for the late 1980s. Indeed, Østerhus and Gammelsrød (1999) found in late 1992 a weak flow into the Greenland basin. However, from 1998 onwards a clear and consistent deep inflow from the Norwegian into the Greenland basin is found in the model, suggesting a deep re-circulation arm within the southern part of the Nordic Seas consistent with the increase in the deep East Icelandic Current and the changes in the model's density in the deep Greenland basin. In contrast, the Labrador Current undergoes severe weakening at all depths (figure 9), as part of the decline of the North Atlantic's sub-polar gyre.

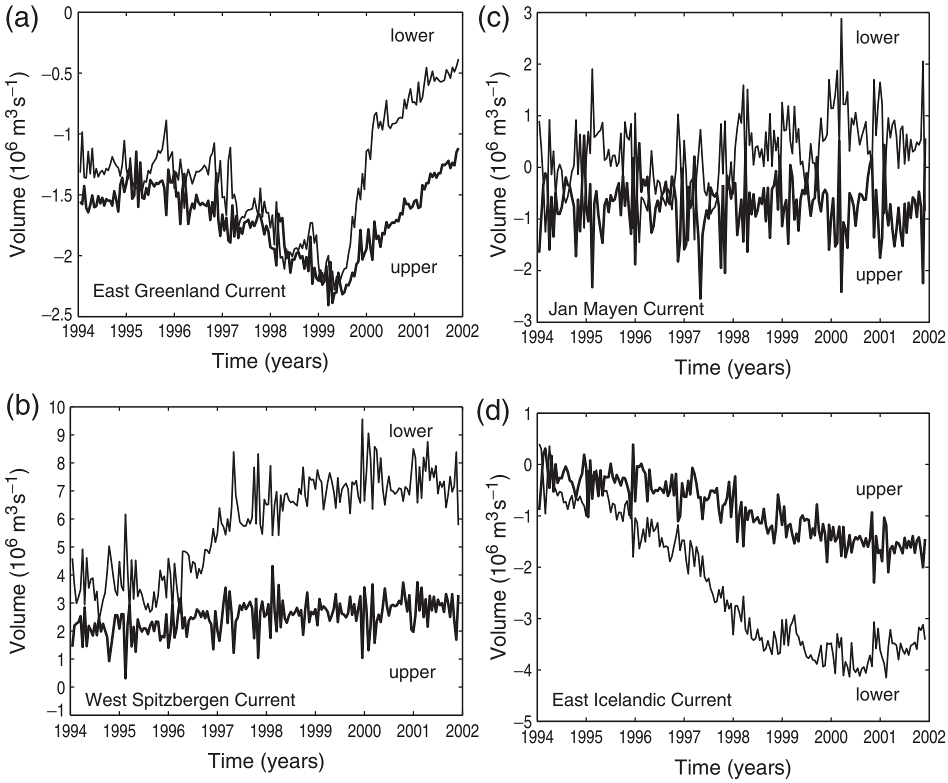

Figure 6. Volume fluxes (in Sv), with a 1 month running mean, within principal currents internal to Nordic Seas: (a) East Greenland Current, (b) West Spitzbergen Current, (c) Jan Mayen Current and (d) East Icelandic Current. The boundary between the upper and lower layers of each is taken at ~150 m, with the lower layer line thinner. Currents in (b)–(d) are from the northern, central and southern thirds respectively of the section from Svalbard to Iceland shown in figure 1(b).

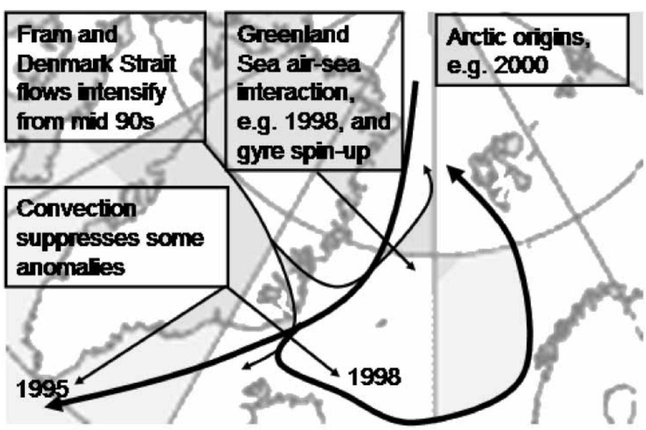

Figure 7. Schematic of circulation changes in the Nordic Seas during the 1990s.

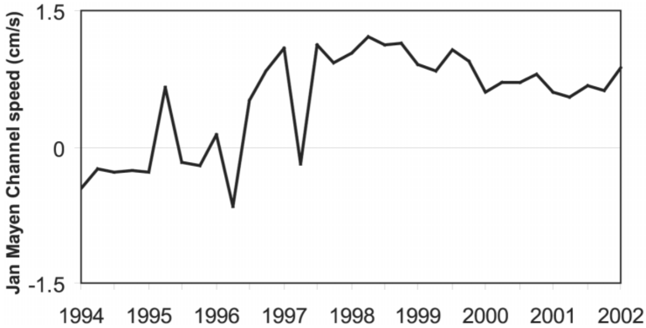

Figure 8. Timeseries of the average speed of the flow (cm s^{-1}) through the bottom model level within the Jan Mayen Channel, using quarterly means.

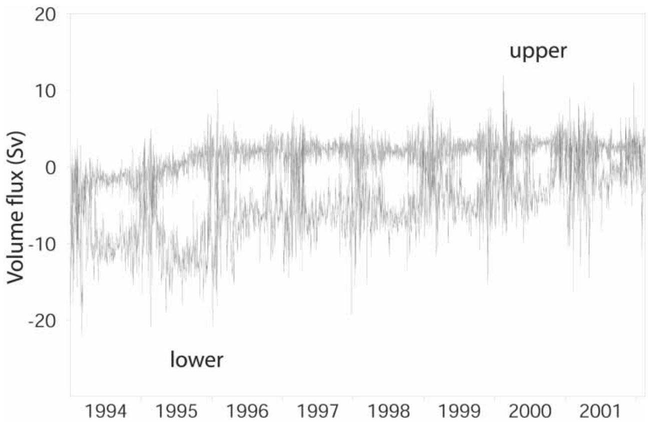

Figure 9. Volume flux (in Sv) in the Labrador Current. The upper and lower layers are taken at ~150 m.

4. Comparison of model and observations

The discussion in the Introduction highlights ten points where model and observations can be compared. These are shown in table 1, with the result of the comparison. The rest of this section discusses these comparisons, leading to the synthesis of the model's contribution to our understanding of how the Nordic Seas behaved during 1994–2001.

4.1. *Key comparisons*

One of the most significant changes to occur to the northern Atlantic during the 1990s was the re-arrangement of convection locations. Deep convection formerly occurred in the Labrador Sea, with significant convection also in the Irminger Sea (Pickart *et al*. 2003). The former began shallowing after 1994 (Lazier *et al*. 2002), reaching an equilibrium by 1998. In the model a maximum in convection occurs in both the Labrador (figure 10) and Irminger Seas during 1994–1997, associated with an increase in salinity (seen in the west Irminger Sea and deep Labrador Sea

Table 1. Comparison of model and observations.

	Observation	Model test	Result
1	Convection depth shallows in Labrador Sea after 1994	Profiles in centre of Labrador Sea	Convection in 1994 to ~1500 m, deepens in 1994–1997 and then shallows to ~1000 m
2	Greenland Sea convection deepens sometime after 1994	Profiles in centre of Greenland Sea	Deep convection, ~2000 m, until early 1999, after which T, S and ρ decline. Note Norwegian Sea convection from spring 2000 to ~2000 m
3	Warming in the abyssal Nordic Seas	Deep temperature of each basin	Bottom of each basin warmed slightly
4	Warming and salinification of LSW	T & S profiles in centre of Labrador Sea	S & T low in 1994, then both increasing, S through 1997, T through 1999. Trend then reverses
5	Sea-ice extent in Greenland Sea increases in later 1990s	Greenland Sea sea-ice volume	Ice cover increases from 1997 on, with maximum in 2000 and little loss in summer 2000
6	Freshening of water north of Iceland	Profile in centre of Icelandic Sea	Whole depth of Icelandic Sea freshens and cools from 1996, as total convection occurs from winter 1997/98 until 1999/2000
7	S & T maxima during 1998/99 in Denmark Strait	T, S at 63°N, Denmark Strait flux	Salty, warm pulse in 1998/99
8	Increase in Irminger Sea T & S in late 1990s	Profiles in centre of Irminger Sea	Upper Irminger Sea warmed and salinified in late 1990s; deep convection until 1997
9	Palace Float circulation	Model velocity ~1500 m	Model velocity similar to Palace float paths during 1998 at 1500–1800 m
10	Atlantic water inflow minimum in late 1990s	Faroe-Shetland Channel flux	Little long term variability

by Dickson *et al.* 2002). This is followed by a rapid decrease in convection depth to ~1000 m, as the Labrador Sea freshens (again, as found by Dickson *et al.* 2002). Some evidence of a re-deepening to ~1800 m is seen in the model towards the end of the run. Within the Nordic Seas the model shows convection to ~1800 m occurring in different basins at different times. Observations have noted local evidence for deep convection in the Greenland Sea (Gascard *et al.* 2002, Wadhams *et al.* 2002); the model has its most persistent deep convection in the Icelandic Sea (1995–2001) and the Norwegian Sea (1996–2002) while model Greenland Sea convection shallows to ~1200 m from 1999 because of a dramatic cooling and freshening that begins in that year (figure 11). Despite the convection the abyssal waters of both the Greenland and Norwegian basin have warmed, and become slightly saltier, over the model run, as in observations.

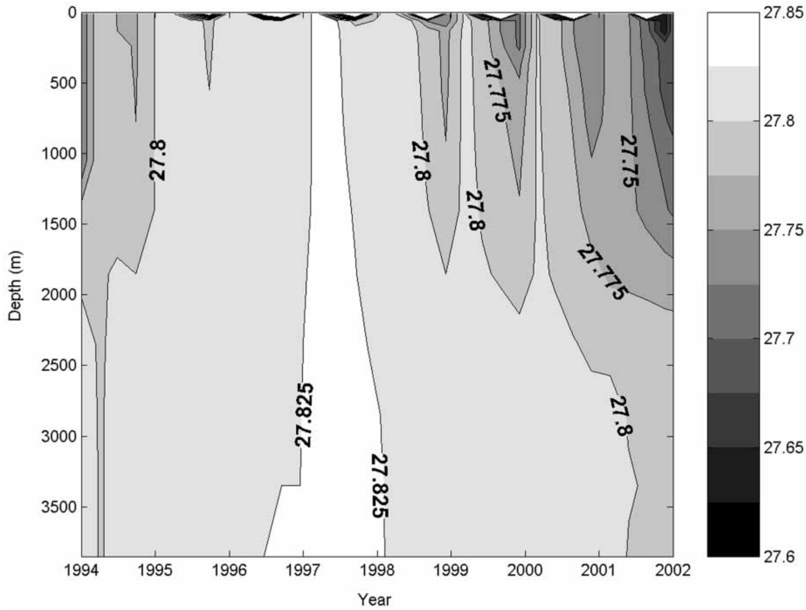

Figure 10. Density profile with time in the centre of the model Labrador Sea.

The Denmark Strait is a pivotal location for the model's circulation. Observational evidence has suggested fresh waters from the East Greenland Current being entrained in the East Icelandic Current during the mid 1990s and again around 2000 (http://www.hafro.is/Sjora/index.htm). The model also shows freshening in this region (figure 11) stemming from the Greenland Sea, although to a greater degree than in the observations. In the model this freshening and cooling propagates into the Norwegian Sea, without the late 1990s break seen in the observations. The early stages of this, at least, are seen at OWS Mike (Dickson *et al.* 2003). This earlier freshening has been ascribed to propagation of a 1990s 'Great Salinity Anomaly' (Belkin 2004). In contrast, it is well known that the Great Salinity Anomaly of the 1960s and 1970s appeared to propagate through the Denmark Strait into the Atlantic, returning to the Norwegian Sea through the Faroe-Shetland Channel some 7 years later (Dickson *et al.* 1999). Dickson *et al.* (2002, 2003) show propagation of anomalies through the Denmark Strait into the Labrador Sea: cool, fresh anomalies leaving the Denmark Strait in 1995 and 1999/2000 and a warm salty one in 1996–1998. The model similarly shows this sequence of anomalies, flowing from the Greenland Sea through the Denmark Strait to the Irminger Sea, where it is most visible as a feature at surface and intermediate water depths (figure 12 and table 1, comparison 7).

The sea-ice flux through Fram Strait is linked to these salinity anomalies propagating around the gyre and out into the Atlantic. Vinje (2001) shows peaks in flux in 1995, 1997/98 and 2000 with minima in 1996 and 1999, broadly agreeing with the general sea-ice pattern for the Greenland Sea observed by satellite (http://polar.wwb.noaa.gov/seaice/Historical.html). The general Northern Hemisphere (and hence Arctic) sea-ice cover decreased through the model run, probably partly in response to a longer-term adaptation to the daily forcing regime. However, the smaller sea-ice volume in the model Greenland Sea has a totally different character,

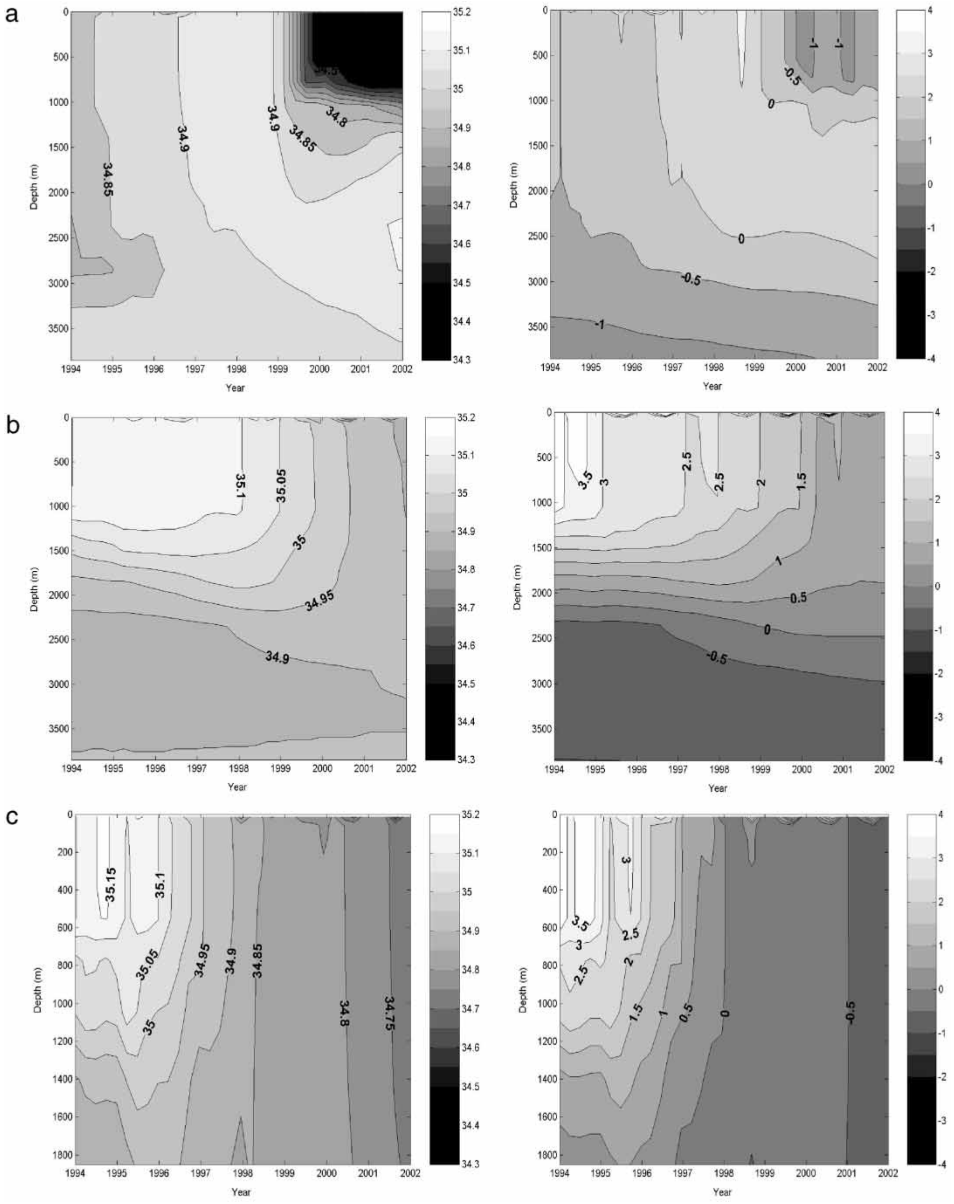

Figure 11. Salinity (left) and temperature (right) temporal profiles in the centre of the (a) Greenland, (b) Norwegian and (c) Icelandic Seas.

with a strong peak in 2000 following a steady rise from 1996 (figure 13). This behaviour follows distinct minima in salinity in the upper waters of the model's Fram Strait in 1996 and 1998/99. The model fresh anomaly seen eventually in the Denmark Strait in 1999/2000 therefore has an Arctic, and sea-ice, origin, in contrast to that in 1995.

A weakness of CONTROL that also occurs in DAILY is the degree to which AW penetrates into the Norwegian Sea. Comparison of upper ocean temperature and salinity with the World Ocean Atlas climatology shows that the model is consistently

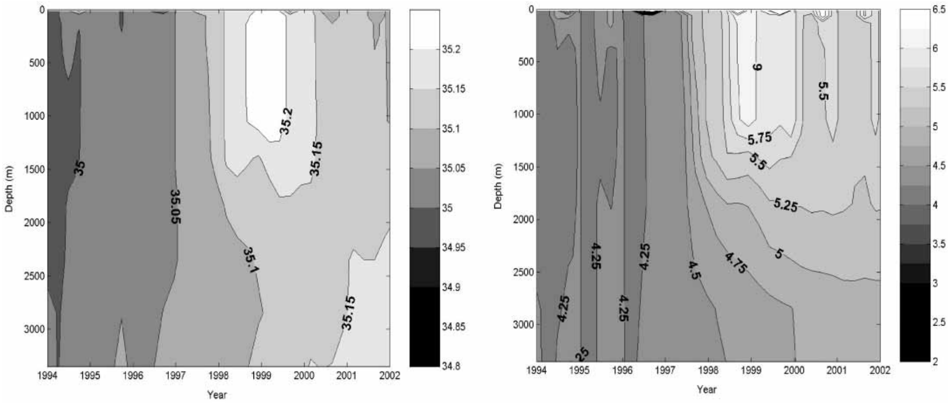

Figure 12. Salinity (left) and temperature (right) temporal profiles in the centre of the Irminger Sea.

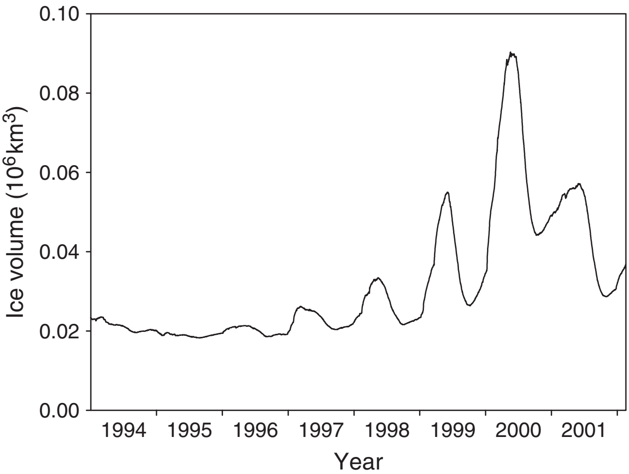

Figure 13. Sea-ice volume integrated over the Greenland Sea (in $10^6\,km^3$).

cooler and fresher in the northern Norwegian Sea. This is because the AW enters the Arctic preferentially through the deeper levels of the Fram Strait in the model, rather than through the Barents Sea. Nevertheless, the basic West Spitzbergen Current supplying this AW is similar in the model to observations. Fahrbach *et al.* (2001) measured 9.5 ± 1.4 Sv in this current during 1997–1999 and Cisewski *et al.* (2003) observed 2–7 Sv in 1997. DAILY also had a spring maximum and summer minimum, with $\sim$8 Sv on average, but fluctuations up to a similar magnitude. However, the magnitude of the East Greenland current only approached 5 Sv in DAILY during the time when the observations gave a southward flow of 11.1 ± 1.7 Sv (Fahrbach *et al.* 2001). Thus observations show a net southward flux through Fram Strait of 4.2 ± 2.3 Sv during this time, but DAILY has 2–3 Sv of net northward flow. Similarly, as the AW preferentially flows into the Arctic through Fram Strait the mean flux through the Barents Sea is $\sim$1.5 Sv out of the Arctic instead of in (Schauer *et al.* 2002). This may be due to the lack of directed river run-off, but also the relatively eastern position of the model section (figure 3).

The modelled inflow into the Nordic Seas through the Faroe-Shetland Channel has a winter peak, with a base summer level of ~4 Sv rising to a peak of 8 Sv during maximum flow in the winter. This remained relatively stable through the period of integration, apart from a weakened inflow in the winter of 1995–1996. This flow is similar to the 7.6 Sv observed further north on the Svinoy section during 1995–1999 by Orvik *et al.* (2001). They also found an absence of a seasonal cycle through 1995–1996, when the NAO briefly, but dramatically, reversed.

4.2. *The overflow paths*

Dickson *et al.* (2002) showed that there has been a rapid freshening of the deep overflow from the Nordic Seas into the Northern Atlantic in recent decades. However, there is a significant interannual variability in this signal, especially in the 1990s. The temperature record from the sites used by Dickson *et al.* (2002) shows a similar variability during the 1990s. In general, the deep overflow in the model captures the trends in both temperature and salinity up to around 1999, although in some places over-estimating the magnitude of the change. However, the last few years of the simulation see more divergence between model and observations. This later discrepancy is clearer in the Denmark Strait Overflow, downstream of the Denmark Strait itself (figure 14). On the other overflow route, through the FSC, the match of model to observations downstream within the Icelandic basin is quite good, but the salinity trends, in particular in the FSC itself, are not well described. However, the physics of downslope flow and deep mixing is not well represented within even fine resolution models, so good agreement is unlikely. The model run is also insufficiently long for signals to have propagated throughout the northern Atlantic.

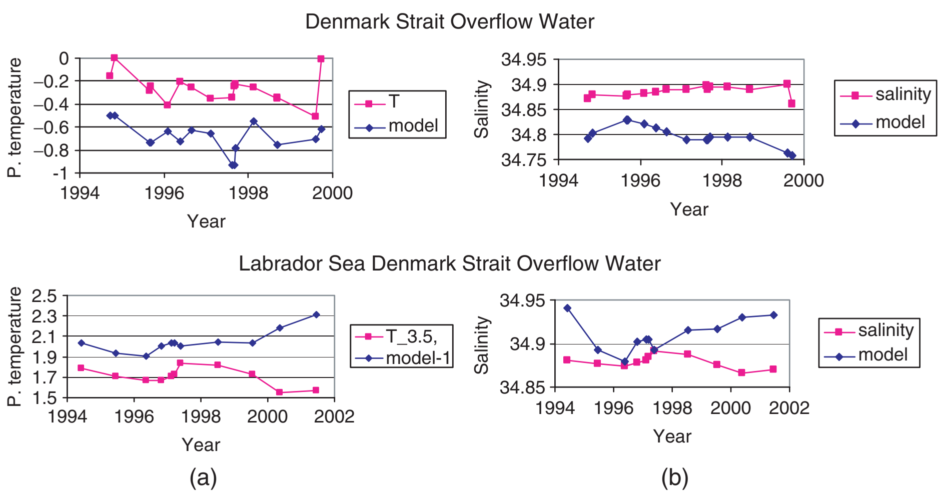

Figure 14. Comparison of daily model (a) potential temperature and (b) salinity with observational timeseries of overflow water from the Denmark Strait (see figure 1(b) of Dickson *et al.* (2002) for location of data). The model gridpoint and level is closest to that of the appropriate observational timeseries. In the Labrador Sea the potential temperature is referenced to 3500 m. Model data (diamonds) have been interpolated from seasonal dumps to the time for the observational data (squares).

5. Discussion

The overall picture of the evolution of the Nordic Seas circulation through the 1990s from the model is therefore as follows. A period of stability in the early 1990s ended in late 1995, accompanying the concurrent change in atmospheric circulation signalled by an abrupt reversal of the North Atlantic Oscillation in the winter of 1995/96. Convection then began to increase, with a concomitant increase in the strength of all parts of the Nordic Seas gyre circulation. This includes an increase in flux out of the Arctic through Fram Strait, into the East Greenland Current, Denmark Strait and East Icelandic Current and an increase in the West Spitzbergen Current at depth. There was also an increase in sea-ice in the Greenland Sea while the Arctic cover reduced, although part of this may have been an adjustment of the model to the NCEP fluxes. In contrast, the sub-polar gyre in the northern Atlantic weakened. These trends continued until late 1997–1998, at which time most components of the circulation stabilised at new values. Nevertheless, the flow continued to strengthen through the Denmark Strait and in the upper part of the East Icelandic Current, although the coastal part of the East Greenland Current upstream weakened. The deep outflow through the FSC also began to weaken at this time, although the inflow into the Nordic Seas remained at a similar strength throughout the simulation. This weakening outflow coincides with a reversal of the deep flow through the Jan Mayen Channel. Note also that the Atlantic overturning also began to weaken at this time, as the Labrador Current declined significantly. Overall, through 1993–2001, the model suggests that the northern Atlantic and adjacent seas adjusted to the change in atmospheric state following the decline of the record NAO Index in 1995 within 2–3 years in most areas, but with some parts of the system continuing to evolve beyond 1998.

Within this record of model flow adjustment to the post-1994 atmosphere, two fresh water anomalies were observed in the Greenland Sea, in 1995 and 1999/2000 and a warm salty one in 1996–1998. All of these exited through the Denmark Strait leaving a clear imprint in the Irminger Sea but, apart from the last, fresh, anomaly, a reduced signal in the Labrador Sea. The model's fresh water anomalies are also seen to propagate eastwards in the southern part of the Nordic Sea gyre, past northern Iceland into the Norwegian Sea. The warm anomaly is not detected on this route; it is presumably mixed out by the deep convection in the Icelandic Basin. The later fresh anomaly of 1999/2000 has clear precursors in flow from the Arctic through Fram Strait, and increased sea-ice in the Greenland Sea. The model clearly ascribes this to an Arctic, and sea-ice, origin. However, while weak signals of both the previous anomalies, salty and fresh, can be detected in Fram Strait, air–sea interaction downstream has amplified them considerably within the Greenland Sea itself. While the model spin-up will have affected the 1995 signal, atmospheric conditions were sufficient to generate these anomalies within the Greenland Sea, without a strong coupling to the model's sea-ice volume. Anomalies within the East Greenland Current do not, therefore, have to be associated with Arctic and sea-ice anomalies, but may be generated by air–sea interaction internal to the Greenland Sea.

The model has general similarities to a significant number of features of the observational record (table 1), but in places tends to diverge in the later years of the record, and generally shows too much freshening, and possibly volume transport, in several regions. This is most noticeable in some parts of the overflow, indicating that too much deep water formation may be occurring in the model. The enhanced volume fluxes may be due to the known over-estimation of air–sea heat fluxes of the NCEP re-analysis due to the atmospheric surface layer parameterisation (Moore and Renfrew 2002, Renfrew *et al.* 2002), the poor precipitation fluxes (Sathiyamoorthy and Moore 2002) or the resolution of the NCEP re-analysis (Moore 2003). Nevertheless, the model illustrates well the possibility for anomalies within the Nordic Seas to both propagate through the Denmark Strait into the Atlantic, and for anomalies to be part of a strong re-circulation signal within the Nordic Seas themselves. On both routes the model suggests that signals can be quickly degraded, through convective mixing. The model shows the potential for oceanic signals of Arctic origin to propagate into the Atlantic, but also for air–lsea interaction within the Nordic Seas to be capable of generating significant anomalies independent of the Arctic. The model also shows that forcing at a realistic daily timescale produces pronounced sub-decadal variability in both major and minor facets of the ocean circulation.

Acknowledgements

This work was funded by the NERC COAPEC Programme (Grant NER/T/S/2000/00334). NCEP Reanalysis data was provided by the NOAA-CIRES Climate Diagnostics Center, Boulder, Colorado, USA, from their web site at http://www.cdc.noaa.gov/. SRD was supported by DEFRA contracts AE1222, AE1225 and the ASOF(W) Project of the European Community Framework V Programme. Two anonymous referees helped make the article more readable.

References

Arfeuille, G., Mysak, L.A. and Tremblay, L.B., 2000, Simulation of the interannual variability of the wind-driven Arctic sea-ice cover during 1958–1998. *Journal of Climate*, **16**, pp. 107–121.

Beare, M.I., 1998, The Southampton-East Anglia Parallel Ocean Circulation Model: Equations and finite difference scheme. Available online at www.mth.uea.ac.uk/ocean/SEA/.

Belkin, I.M., 2004, Propagation of the "Great Salinity Anomaly" of the 1990s around the northern North Atlantic. *Geophysical Research Letters*, **31**, doi:10.129/2003GL08306.

Bourke, R.H., Paquette, R.G., Blythe, R.F. and Stone, M.D., 1993, On the deep and bottom waters of the Greenland Sea from summer 1989 and 1990 data. *Journal of Geophysical Research-Oceans*, **98**, pp. 4629–4638.

Cisewski, B., Budéus, G. and Krause, G., 2003, Absolute transport estimates of total and individual water masses in the northern Greenland Sea derived from hydrographic and acoustic Doppler current profiler measurements. *Journal of Geophysical Research-Oceans*, **108**, doi:10.1029/2002JC001530.

Comiso, J.C., Wadhams, P., Pedersen, L.T. and Gersten, R.A., 2001, Seasonal and interannual variability of the Odden ice tongue and a study of environmental factors. *Journal of Geophysical Research-Oceans*, **106**, pp. 9093–9116.

Dickson, B., Meincke, J., Vassie, I., Jungclaus, J. and Østerhus, S., 1999, Possible predictability in overflow from the Denmark Strait. *Nature*, **397**, pp. 243–246.

Dickson, B., Yashayaev, I., Meincke, J., Turrell, B., Dye, S. and Holfort, J., 2002, Rapid freshening of the deep North Atlantic Ocean over the past four decades. *Nature*, **416**, pp. 832–837.

DICKSON, R.R., CURRY, R. and YASHAYAEV, I., 2003, Recent changes in the North Atlantic. *Philosophical Transactions of the Royal Society Series A*, **361**, pp. 1917–1933.

DYE, S.R., 1999, A century of variability of flow through the Faroe-Shetland Channel. PhD thesis, University of East Anglia.

ENGLAND, M.H., 1993, Representing the global-scale water masses in ocean general circulation models. *Journal of Physical Oceanography*, **23**, pp. 1523–1552.

ETOPO, 1986, *Global* $5' \times 5'$ *Depth and Elevation* (Boulder, U.S.A: National Geophysical Data Center, NOAA).

FAHRBACH, E., MEINCKE, J., ØSTERHUS, S., ROHARDT, G., SCHAUER, U., TVERBERG, V. and VERDUIN, J., 2001, Direct measurements of volume transports through Fram Strait. *Polar Research*, **20**, pp. 217–224.

FUREVIK, T., 2001, Annual and interannual variability of Atlantic Water temperature in the Norwegian and Barents Seas: 1980–1996. *Deep-Sea Research Part I*, **48**, pp. 383–404.

GASCARD, J.-C., WATSON, A.J., MESSIAS, M.-J., OLSSON, K.A., JOHANNESSEN, T. and SIMONSEN, K., 2002, Long-lived vortices as a mode of deep ventilation in the Greenland Sea. *Nature*, **416**, pp. 525–527.

GRIFFIES, S.M., GNANDESIKAN, A., PACANOWSKI, R.C., LARICHEV, V., DUKOWICZ, J.K. and SMITH, R.D., 1998, Iso-neutral diffusion in a z-coordinate ocean model. *Journal of Physical Oceanography*, **28**, pp. 831–841.

HELLERMAN, S. and ROSENSTEIN, M., 1983, Normal monthly wind stress over the world's ocean with error estimates. *Journal of Physical Oceanography*, **13**, pp. 1093–1104.

KALNAY, E., KANAMITSU, M., KISTLER, R., COLLINS, W., DEAVEN, D., GANDIN, L., IREDELL, M., SAHA, S., WHITE, G., WOOLLEN, J., ZHU, Y., CHELLIAH, M., EBISUZAKI, W., HIGGINS, W., JANOWIAK, J., MO, K.C., ROPELEWSKI, C., WANG, J., LEETMAA, A., REYNOLDS, R., JENNE, R. and JOSEPH, D., 1996, The NCEP/NCAR 40-year reanalysis project. *Bulletin of the American Meteorological Society*, **77**, pp. 437–471.

KARCHER, M.J., GERDES, R., KAUKER, F. and KOBERLE, C., 2003, Arctic warming: evolution and spreading of the 1990s warm event in the Nordic seas and the Arctic Ocean. *Journal of Geophysical Research-Oceans*, **108(C2)**, doi: 10.129/2001JC001265, art. no. 3034.

KILLWORTH, P.D., 1995, Time interpolation of forcing fields in ocean models. *Journal of Physical Oceanography*, **26**, pp. 136–143.

LABRADOR SEA GROUP, 1998, The Labrador Sea deep convection experiment. *Bulletin of the American Meteorological Society*, **79**, pp. 2033–2058.

LAZIER, J., HENDRY, R., CLARKE, A., YASHAYAEV, I. and RHINES, P., 2002, Convection and restratification in the Labrador Sea, 1990–2000. *Deep-Sea Research Part I*, **49**, pp. 1819–1835.

LEVITUS, S. and BOYER, T.P., 1994, *World Ocean Atlas, Volume 3: Salinity* (Washington D.C.: NOAA).

LEVITUS, S., BURGETT, R. and BOYER, T.P., 1994, *World Ocean Atlas, Volume 4: Temperature*. (Washington DC: NOAA).

LHERMINIER, P., GASCARD, J.-C. and QUADFASEL, D., 1999, The Greenland Sea in winter 1993 and 1994: preconditioning for deep convection. *Deep-Sea Research Part II*, **46**, pp. 1199–1235.

MALMBERG, S.A. and JONSSON, S., 1997, Timing of deep convection in the Greenland and Iceland Seas. *ICES Journal of Marine Science*, **54**, pp. 300–309.

MOORE, G.W.K., 2003, Gale force winds over the Irminger Sea to the east of Cape Farewell, Greenland. *Geophysical Research Letters*, **30**, doi:10.129/2003GL018012, art. no. 1894.

MOORE, G.W.K. and RENFREW, I.A., 2002, An assessment of the surface turbulent heat fluxes from the NCEP-NCAR reanalysis over the western boundary currents. *Journal of Climate*, **15**, pp. 2020–2037.

OBERHUBER, J.M., 1988, An atlas based on the COADS data set: the budgets of heat, buoyancy and turbulent kinetic energy at the surface of the global ocean. *Report 15*, Max-Planck-Institut fur Meteorologie, Hamburg, Germany.

ORVIK, K.A., SKAGSETH, O. and MORK, M., 2001, Atlantic inflow to the Nordic Seas: current structure and volume fluxes from moored current meters, VM-ADCP and SeaSoar-CTD observations 1995–1999. *Deep-Sea Research Part I*, **48**, pp. 937–957.

ØSTERHUS, S. and GAMMELSRØD, T., 1999, The abyss of the Nordic Seas is warming. *Journal of Climate*, **12**, pp. 3297–3304.

ØSTERHUS, S., TURRELL, W.R., JÓNSSON, S. and HANSEN, B., 2005. Measured volume, heat, and salt fluxes from the Atlantic to the Arctic Mediterranean. *Geophysical Research Letters*, **32**, doi:10.129/2004GL022188, art. no. L07603.

PARKINSON, C.L. and WASHINGTON, W.M., 1979, A large-scale numerical model of sea ice. *Journal of Geophysical Research*, **84**, pp. 311–337.

PHILANDER, S.G.H. and PACANOWSKI, R.C., 1986, A model of the Seasonal Cycle in the Tropical Atlantic-Ocean. *Journal of Geophysical Research – Oceans*, **91**, pp. 14192–14206.

PICKART, R.S., SPALL, M.A., RIBERGAARD, M.H., MOORE, G.W.K. and MILLIFF, R.F., 2003, Deep convection in the Irminger Sea forced by the Greenland tip jet. *Nature*, **424**, pp. 152–156.

RENFREW, I.A., MOORE, G.W.K., GUEST, P.S. and BUMKE, K., 2002, A comparison of surface layer and surface turbulent flux observations over the Labrador Sea with ECMWF analyses and NCEP reanalyses. *Journal of Physical Oceanography*, **32**, pp. 383–400.

REVERDIN, G., VEBRUGGE, N. and VALDIMARSSON, H., 1999, Upper ocean variability between Iceland and Newfoundland, 1993–1998. *Journal of Geophysical Research-Oceans*, **104**, pp. 29599–29611.

RHEIN, M., FISCHER, J., SMETHIE, W.M., SMYTHE-WRIGHT, D., WEISS, R.F., MERTENS, C., MIN, D.H., FLEISCHMANN, U. and PUTZKA, A., 2002, Labrador Sea Water: Pathways, CFC inventory, and formation rates. *Journal of Physical Oceanography*, **32**, pp. 648–665.

SATHIYAMOORTHY, S. and MOORE, G.W.K., 2002, Buoyancy flux at Ocean Weather Station Bravo. *Journal of Physical Oceanography*, **32**, pp. 458–474.

SCHAUER, U., LOENG, H., RUDELS, B., OZHIGIN, V.K. and DIECK, W., 2002, Atlantic water flow through the Barents and Kara Seas. *Deep-Sea Research Part I*, **49**, pp. 2281–2298.

SCHMITH, T. and HANSEN, C. 2003, Fram Strait ice export during the 19th and 20th centuries reconstructed from a multi-year sea-ice index from Southwestern Greenland. *Journal of Climate*, **16**, pp. 2782–2791.

THOMPSON, S.R., 1995, Sills of the global ocean: a compilation. *Ocean Modelling*, **109**, pp. 7–9 (Unpublished manuscript).

TOUDAL, L., 1999, Ice extent in the Greenland Sea 1978–1995. *Deep-Sea Research Part II*, **46**, pp. 1237–1254.

TURRELL, W.R., SLESSER, G., ADAMS, R.D., PAYNE, R. and GILLIBRAND, P.A., 1999, Decadal variability in the composition of Faroe-Shetland Channel bottom water. *Deep-Sea Research Part I*, **46**, pp. 1–25.

VINJE, T., 2001, Fram Strait ice fluxes and atmospheric circulation: 1950–2000. *Journal of Climate*, **14**, pp. 3508–3517.

WADHAMS, P., HOLFORT, J., HANSEN, E. and WILKINSON, J.P., 2002, A deep convective chimney in the winter Greenland Sea. *Geophysical Research Letters*, **29**(10), doi: 10.129/2001GL014306, art. no. 1434.

WADLEY, M.R. and BIGG, G.R., 2000, Implementation of variable time stepping in an ocean general circulation model. *Ocean Modelling*, **1**, pp. 71–80.

WADLEY, M.R. and BIGG, G.R., 2002, Impact of flow through the Canadian Archipelago and Bering Strait on the North Atlantic and Arctic circulation: an ocean modelling study. *Quarterly Journal of the Royal Meteorological Society*, **128**, pp. 2187–2203.

WEBB, D.J., 1996, An ocean model code for array processor computers. *Computational Geosciences*, **22**, pp. 569–578.